ISSN (Print) : 0974-6846
ISSN (Online) : 0974-5645
Indian Journal of Science and Technology, *Vol 9(41), DOI: 10.17485/ijst/2016/v9i41/101971, November 2016*

Mechanical Properties and Phase Transformations in Resistance Spot Welded Dissimilar Joints of AISI409M/AISI301 Steel

A. Subrammanian[1]*, D. B. Jabaraj[2], J. Jayaprakash[3] and V.K. Bupesh Raja[4]

[1]Department of Mechanical Engineering, St Peters University, Avadi, Chennai- 600054, Tamil Nadu, India; prakash221271@gmail.com
[2]Dr MGR Educational and Research Institute University, Chennai - 600095, Tamil Nadu, India; jabaraj2009@yahoo.com
[3]Department of Mechanical Engineering, Dr MGR Educational and Research Institute University, Chennai - 600095, Tamil Nadu, India; profjaya@gmail.com
[4]Department of Automobile Engineering, Sathyabama University, Chennai - 600119, Tamil Nadu, India; bupeshvk@gmail.com

Abstract

Objectives: In this study, the mechanical properties and phase transformations of resistance spot welded dissimilar joints between austenitic stainless steel AISI 301 and ferity stainless steel AISI 409M are investigated. **Methods/Analysis:** Mechanical properties such as tensile shear strength, failure energy, failure mode, nugget size and surface indentation were analysed at varying current ratings. Macrostructure was examined for size and shape. Microstructure at various locations such as, fusion zone and heat affected zones were investigated. Micro hardness measurement was done at various locations along the weld. **Findings**: Tensile shear strength increases with increase in welding current in expulsion free welds. Fusion zone hardness was found to be larger than that of both base metals and heat affected zones. Nugget size and energy absorbing capacity of the spot weld were found to be in correlation with weld current in expulsion free samples. Electrode indentation on the nugget surface increases with increase in welding current. Fusion zone microstructure consists of martensite and ferrite. Asymmetrical nugget shape was observed. **Novelty/Improvement:** Investigating the effects of resistance spot welding on the mechanical properties and phase transformations of ferritic-austenitic dissimilar metal weld joint.

Keywords: AISI301, AISI409M, Dissimilar Metal Welding, Resistance Spot Welding, Tensile Shear Strength

1. Introduction

Resistance Spot Welding (RSW)is prominent in joining sheet metal[1]. Both electric current and mechanical pressure are applied together to make joints in RSW process[2]. RSW is an attractive choice for automobile and rail car manufacturing industries, as it is less expensive, faster and can be automated easily. The growth of the weld nugget in RSW is determined by the variables, such as current, weld time, electrode tip size, and force[3].

Ferritic Stainless Steels (FSS) account to nearly half of the AISI 400 series stainless steels. They are considered as cheaper substitutes to austenitic stainless steels[4]. Nowadays, ferritic stainless steel is widely used for auto-

*Author for correspondence

mobile and rail car structuralapplications[5]. Austenitic Stainless Steel (ASS) is used for railcar structural application[6].

Dissimilar metal welding is commonly used in industries nowadays. The quality of such joints will often be vital to the proper functioning of the whole unit. Many research works[7,8] have been reported in the past on dissimilar metal spot welding. However, most of the studies in dissimilar spot welding, dealt with the combination of austenitic stainless steel and any other non stainless steel metal. Reported works on dissimilar metal spot welding between ASS and FSS are limited. Such joints find application in railcar manufacturing industries. A deep understanding about the effect of RSW on the properties of the weld is essential to improve the performance of the joint. Hence, in this work, an effort is made to investigate the mechanical properties and phase transformations of resistance spot welded dissimilar joints between ASS AISI 301 and FSS AISI409M.

2. Materials and Methods

2.1 Material

In this study, 2 mm thick cold rolled sheets of ferritic stainless steel AISI 409M and austenitic stainless steel AISI301 were welded by RSW. Test samples for tensile shear test were made ready, confirming to ISO 14273 standards. The size of the test specimen used in this study is of 60 mm width and 138 mm length. Chemical composition of both the test materials was tested with spectrometer and is shown in Table 1.

2.2 Experimental

The experiment was conducted on a PLC controlled, 75 KVA, pedestal type resistance spot welding machine (make-Jaya Hind Sciaky, model- P252). Truncated electrodes of 45°, with a tip diameter of 8 mm, RWMA class 3, were used for welding. Welding was done with varying current, starting from 7kA(Kilo ampere) to 14 kA with a regular increment of 1kA, keeping electrode force and weld cycle as constants, such as 4 kN (Kilo Newton) and 15 cycles (1 cycle = 20 milliseconds)respectively, based on preliminary trials. Other parameters such as squeeze time hold time and off time were kept constant, as 40 cycles, 20 cycles and 20 cycles respectively.

2.2.1 Mechanical Tests

Tensile shear test was conducted on a universal tensile testing machine (make-TE-JINAN, model no-WDW 100). Tensile shear strength, corresponding to the peak point in the load-displacement curve of tensile test, was recorded for each test sample. The energy absorbed during failure was determined by measuring the area below the load-displacement curve, up to the peak load, of tensile shear test. Mode of failure such as, interfacial mode or pull out mode, in each sample was noted during the tensile shear test. To determine the size of the nugget, peel test was carried out on specimens, welded at varying currents and average diameter of the nugget was recorded, corresponding to each current value. Indentation, the depression made by the electrode tip on the surface of the sheet, has been recorded for each specimen, using a digi-

Table 1. Chemical composition of test materials (percentage by weight)

Grade	C	Si	Mn	P	S	Cr	Cu	Ni	Ti	Al	Fe
AISI 409M	0.030	0.418	0.879	0.028	0.013	12.33	0.014	0.071	0.02	0.014	Balance
AISI 301	0.068	0.693	1.520	0.011	0.018	16.09	0.225	6.009	----	----	Balance

tal depth gauge with an accuracy of 0.01mm, to analyse the effect of current on it .

2.2.2 Metallurgical Study

Specimens for microstructure examination were prepared according to standard metallographic procedure. Etching of the specimens was done with Kalling's No.1 etchant. Microstructure examination was carried out at various locations such as Base Metal (BM), Heat Affected Zones (HAZ) of both the metals and Fusion Zone (FZ) by optical microscopy. Fusion zone size was also measured through microscope using wire cross sections.

Micro hardness was measured by hardness tester, make-Shimadzu, 0.5Kg. Hardness was taken at different locations vertically, covering both the FSS and ASS sides, such as base metal of FSS (BM FSS), low/high temperature heat affected zone (LTHAZ /HTHAZ) of FSS, fusion zone heat affected zone of ASS (HAZ ASS) and base metal of ASS (BM ASS).

2.2.3 Macroscopic Test

Macrograph of spot welded dissimilar joint between ASS and FSS consists of three distinct regions such as BM, HAZ and FZ. Geometrical characteristics such as size and shape of the nugget, amount of penetration of the weld can be obtained from the macrograph.

3. Results and Discussion

3.1 Mechanical Properties

Various output parameters such as tensile shear strength, failure energy, nugget size and micro hardness were measured to investigate the mechanical properties. It was observed that there is a direct correlation between tensile shear strength and current ratings. Scatter plot of tensile shear strength with current is shown in Figure 1. However, it can be seen from the graph that, at higher current values, tensile shear strength does not increase with further increase in current, due to expulsion. Expulsion results in heat and metal loss from the weld, causing reduction in peak load. Fusion zone size increases with increase in current value, due to more heat input and subsequent increased melting of metal. The correlation between nugget diameter and current is given in Figure 2. As in the case of tensile shear strength, nugget diameter ceases to be in direct relationship with current, at high current ratings, due to excessive expulsion. It is well documented in studies in the past, that fusion zone size is one of the most important factor influencing peakload[9,10].

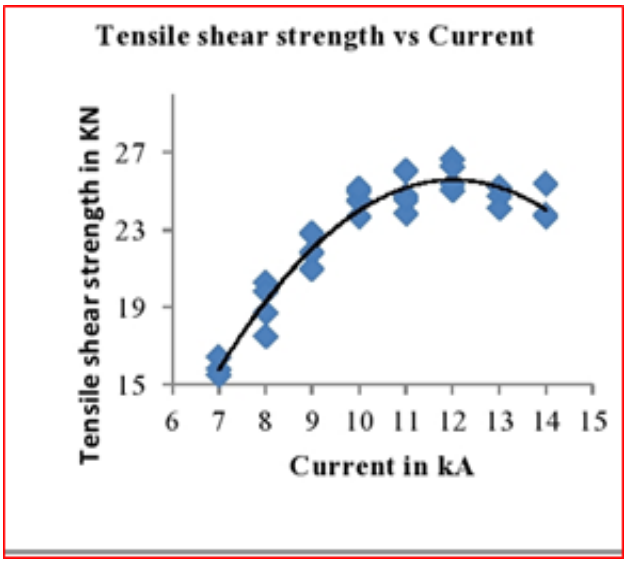

Figure 1. Tensile shear strength-current graph.

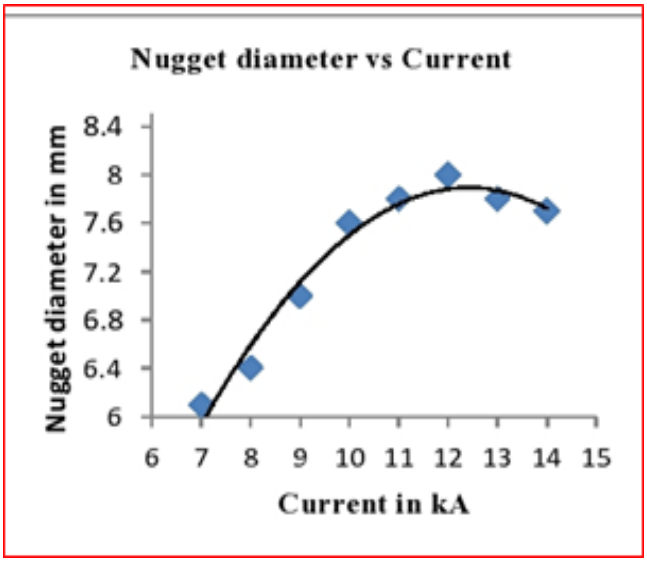

Figure 2. Nugget diameter-current graph.

Failure energy or the energy absorbing capacity of the weld joint also was found to be in direct relationship with current Figure 3. Failure energy in a tensile shear test depends upon the peak load and the displacement during failure. The energy absorption capacity of the weld joint increases with increase in current, primarily, due to increase in fusion zone size. Again it can be noticed that expulsion associated with high welding current results in drop of failure energy.

In spot welding, usually failure occurs in two modes such as, interfacial mode and pull out mode. In interfacial mode, failure occurs by crack propagation along the nugget in a plane parallel to the surface of the sheet, whereas, in pull out mode, complete withdrawal of the nugget from one of the sheet takes place[11,12]. In tensile shear test of dissimilar spot welded joint, test samples welded at a current value of 10 kA and below, failed by interfacial mode and those samples welded with a current above 10 kA, underwent pullout mode of fracture.

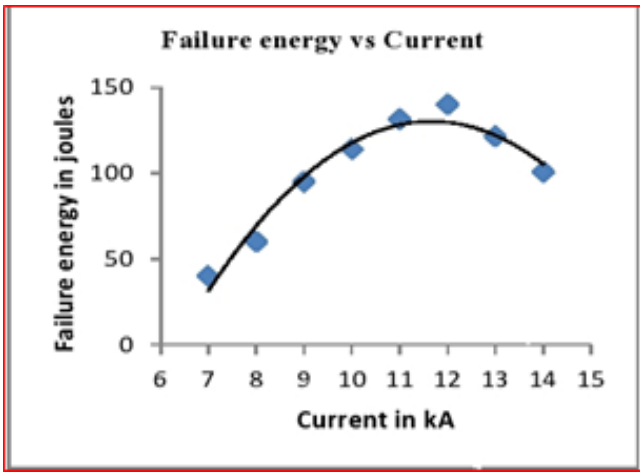

Figure 3. Failure energy- current graph.

Pullout mode of failure is usually preferred over interfacial mode due to the higher tensile shear strength and failure energy associated with the former[12]. Also it was noticed that in all the pull out failures, fracture occurred at the base metal of ASS side, though tensile strength of ASS is more than that of FSS. The HAZ width of ASS was significantly less than that of FSS. Even though, the fusion zone area of ASS is larger than that of FSS, the perimeter of the circle containing both FZ and HAZ in case of ASS is significantly less than that of FSS. As a result, there is a large area of cross section along the thickness of FSS, to resist the external load compared to that of ASS. Therefore, during tensile test, fracture occurred in the ASS base metal.

Indentation values were analysed in relation with the current values. Correlation between indentation and current is given in Figure 4.

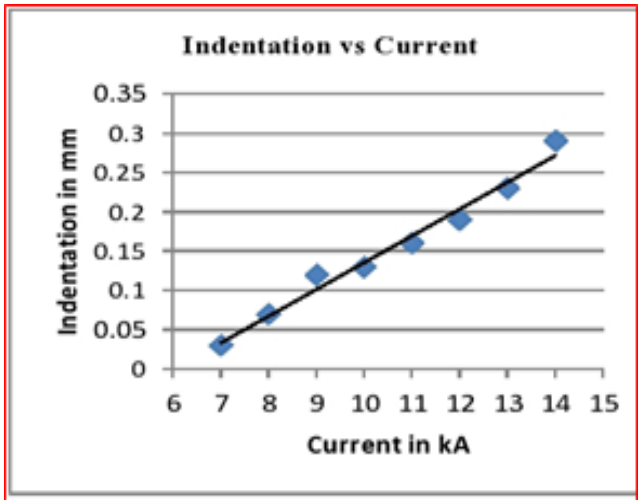

Figure 4. Indentation-current graph.

Increased amount of indentation was noticed with increasing current values. Indentation results in poor surface finish and therefore is not desirable. Increase in current increases the heat input, thereby promotes the plastic deformation at the surface of the sheet, where electrode force is acting. This leads to deeper indentation on the surface of the nugget.

3.2 Macrograph

The macroscopic image of the spot welded joint is given in Figure 5. An asymmetrical nugget shape has been observed, in dissimilar spot welded FSS/ASS joint, with the size of the FZ on ASS side, larger than the other side. The asymmetrical weld nugget in dissimilar metal spot welded joints can be attributed to the differences in ther-

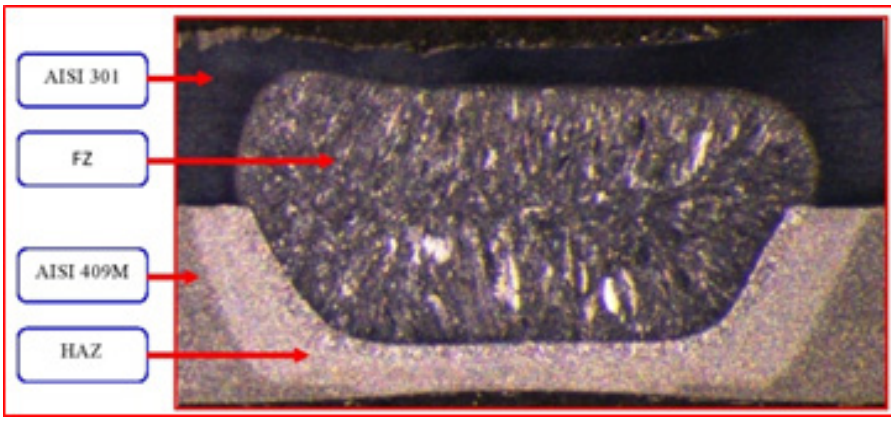

Figure 5. Macrograph of the weld.

mal conductivity and electrical resistivity of the two steel sheets.

3.3 Microstructure

A fully ferritic microstructure was seen in the base metal of FSS Figure 6. In case of ASS base metal, austenite microstructure was noticed Figure 7.

In the HAZ of FSS, while examining the microstructure, two distinct regions were observed Figure 8. The region close to the base metal, where relatively lower temperature prevailed (LTHAZ), consisted of fine grains of ferrite with a small amount of martensite along the grain boundaries whereas the region next to it and close to the fusion zone, where relatively higher temperature prevailed during welding (HTHAZ), consisted of coarse grains of ferrite[13].

As per the Fe-Cr-C pseudo-binary phase diagram[14] for low chromium ferritic stainless steel (13% Cr), the line corresponding to 0.03% carbon content passes mainly through two regions at elevated temperature, as shown in Figure 9. Here the LTHAZ and HTHAZ represent the delta ferrite+austenite ($\delta + \gamma$) and delta ferrite (δ) phase respectively. In the LTHAZ, under elevated temperature, some austenite is formed around the grain boundaries

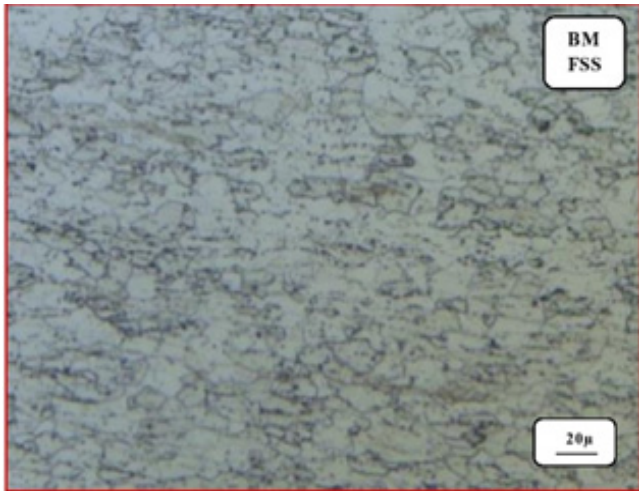

Figure 6. BM FSS microstructure.

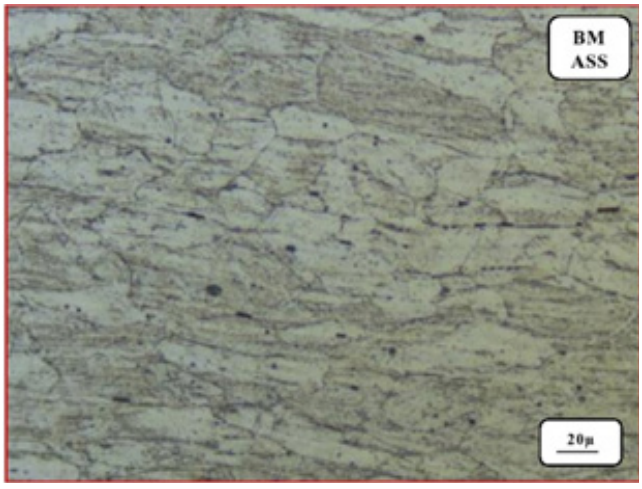

Figure 7. BM ASS microstructure.

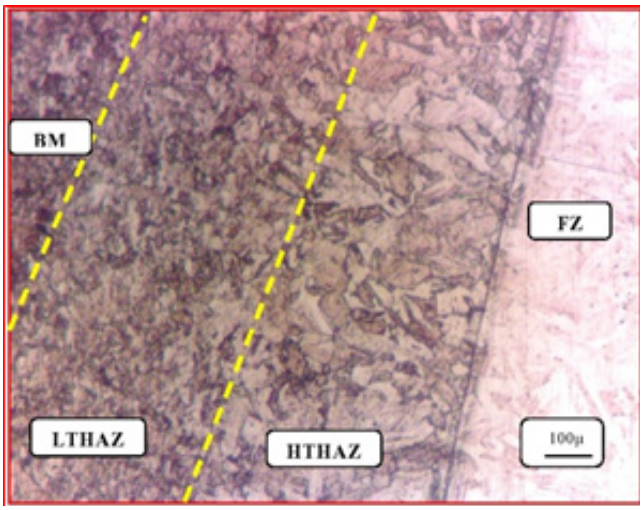

Figure 8. HAZ FSS microstructure.

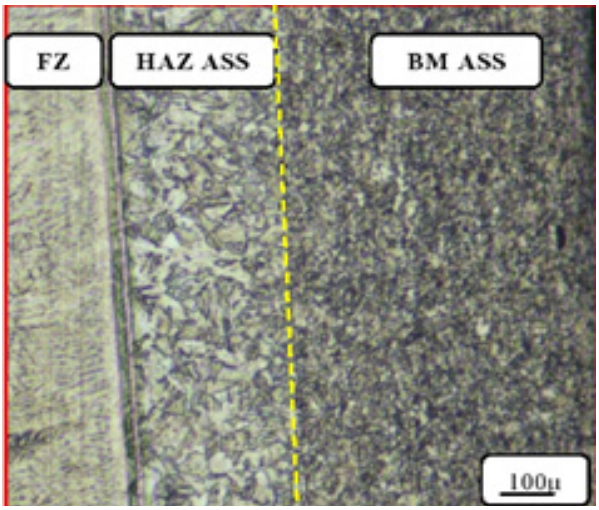

Figure 10. HAZ ASS microstructure.

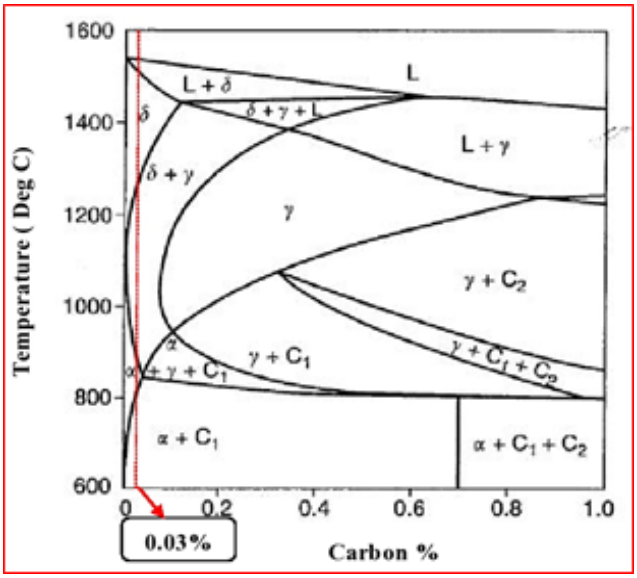

Figure 9. Fe-Cr-C pseudo-binary phase diagram for low chromium ferritic stainless steel (13% Cr) .

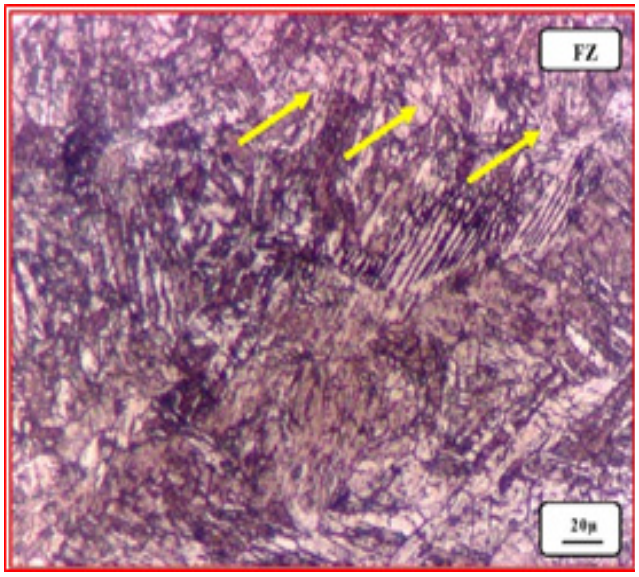

Figure 11. FZ Microstructure, arrow marks shows martensite.

which prevent grain growth in this region. During rapid cooling, that is usually associated with RSW; the same austenite is transformed to martensite and results in increased hardness. In HTHAZ region, at elevated temperature, delta ferrite is formed. However, due to rapid cooling, austenite formation is suppressed and hence the resultant microstructure is fully ferritic, with a fair amount of grain growth. Lower value of micro hardness at this region is in good agreement with its coarse grain ferrite microstructure.

Austenitic microstructure was found in the HAZ of ASS. Though some amount of grain growth could be seen, it was not as large as FSS Figure 10.

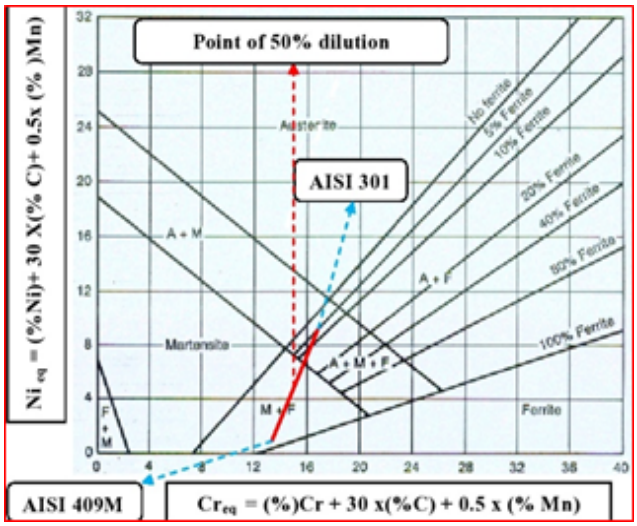

Figure 12. Schaffler diagram to predict the FZ microstructure.

Microstructure of fusion zone was found to be consisting predominantly of martensite and ferrite Figure 11. Microstructure of fusion zone in dissimilar metal welding can be predicted with the help of schaffler diagram. At 50% diffusion, the resultant fusion zone microstructure in the schaffler diagram indicates a combination of ferrite and martensite Figure 12. Higher micro hardness values obtained at fusion zone can be attributed to the presence of martensite.

3.4 Micro Hardness

On analysing the micro hardness values along the cross section of the weld, it was found that the micro hardness at the fusion zone is much higher than that at both the base metals. Micro hardness profile along the weld is shown in Figure 13. Higher micro hardness value of fusion zone with respect to that of BM and HAZ can be attributed to the presence of martensite. Along the HAZ of FSS, micro hardness first increased sharply through the LTHAZ to a maximum and then decreased to a minimum level near to the fusion zone boundary in the HTHAZ. In the LTHAZ of FSS, increasing hardness is mainly due to grain refinement and it steadily increases with the maximum temperature prevailed during the welding. In the HTHAZ, micro hardness values dip due to excessive grain growth related with the absence of high temperature austenite and the rapid cooling rate inherent with resistance spot welding. On the other hand, micro hardness increased steadily along the HAZ of ASS from base metal to fusion zone boundary. Ratio of average fusion zone hardness to FSS base metal hardness was found to be 2.18 approximately and that for ASS base metal was found to be 1.63.

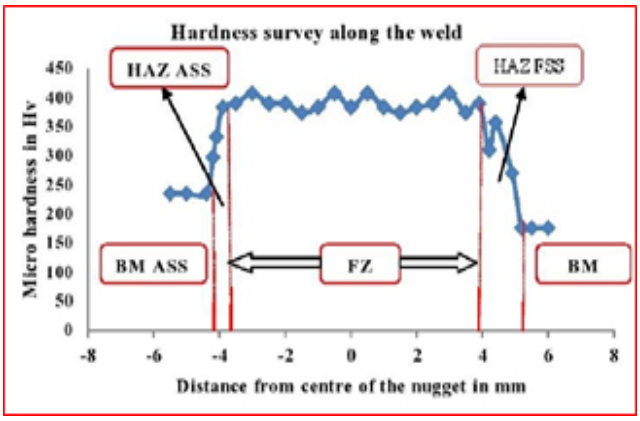

Figure 13. Micro hardness profile of the weld.

4. Conclusions

1. Fusion zone hardness was found to be larger than that of both base metals and heat affected zones.
2. Nugget size and energy absorbing capacity of the spot weld were found to be in correlation with welding current in expulsion free samples. Electrode indentation on the nugget surface increases with increase in welding current.
3. Fusion zone microstructure consists of martensite and ferrite.
4. Asymmetrical nugget shape was observed, with austenitic stainless steel side being larger than ferritic stainless steel side, due to difference in electrical and thermal properties.
5. Grain coarsening was noticed at the high temperature HAZ region, near to the fusion zone boundary.

5. Acknowledgement

Authors are grateful to Advanced Welding Training Institute (AWTI), Integral Coach Factory, Indian Railways, Chennai, India, for extending facilities of Chemical and Metallurgical Testing Laboratory, to carry out this investigation.

6. References

1. Shamsul JB, Hisyam MM. Study of spot welding of austenitic stainless steel type 304. Journal of Applied Sciences Research. 2007 Jan; 3(11):1494-97.
2. Pouranvari M. Effect of welding current on the mechanical response of resistance spot welds of unequal thickness steel sheets in tensile-shear loading condition. International Journal of Multidisciplinary Sciences and Engineering. 2011 Sep; 5(12):63-7.
3. Hamidinejad SM, Kolahan F, Kokabi AH. The modelling and process analysis of resistance spot welding on galvanized steel sheets used in car body manufacturing. Materials and Design. 2012; 34:759-67.
4. Feng JC, Wang YR, Zhang ZD. Nugget growth characteristic for AZ31B magnesium alloy during resistance spot welding. Science and Technology of Welding and Joining. 2006; 11(2):154-62.
5. Pouranvari M, Marashi SPH, Alizadehsh M. Welding metallurgy of dissimilar AISI 430/DQSK steels resistance spot welds. Welding Journal. 2015 Jun; 94(6):203-10.
6. Pouranvari M, Ranjbarnoodeh M. Effect of welding current on energy absorption of AISI 304 resistance spot welds. Research Journal of Applied Sciences Engineering and Technology. 2012 Sep; 4(17):2911-14.
7. Alenius M, Somervuori, Hannien H. Exploring the mechanical properties of spot welded dissimilar joints for stainless and galvanized steels. Welding Journal. 2006 Dec; 85(12):305-13.
8. Marashi P, Pouranvari M, Amirabdollahian S, Abedi A, Goodarzi M. Microstructure and failure behavior of dissimilar resistance spot welds between low carbon galvanized and austenitic stainless steels. Materials Science and Engineering A. 2008 May; 480(1-2):175-80.
9. Pouranvari M. Analysis of fracture mode of galvanized low carbon steel resistance spot welds. International Journal of Multidisciplinary Sciences and Engineering. 2011 Sep; 2(6):36-40.
10. Pouranvari M, Ranjbarnoodeh E. Resistance spot welding characteristic of ferrite-martensite DP600 dual phase advanced high strength steel-part III: mechanical properties. World Applied Sciences Journal. 2011 Jan; 15(11):1521-26.
11. Sun X, Stephens EV, Khaleel MA. Effects of fusion zone size and failure mode on peak load and energy absorption of advanced high strength steel spot welds under lap shear loading conditions. Engineering Failure Analysis. 2008 Jun; 15(4):356-67.
12. Pouranvari M, Asgari HR, Mosavizadeh SM, Marashi PH, Goodarzi M. Effect of weld nugget size on overload failure mode of resistance spot welds. Science and Technology of Welding and Joining. 2007; 12(3):217-25.
13. Subrammanian A, Jabaraj DB, Bupesh Raja VK. Microstructure and mechanical properties of resistance spot welded joints of AISI 409M ferritic stainless steel. Transactions of Indian Institute of Metals. 2016; 69(3):767-74.
14. Lippold JC, Kotecki J. Welding metallurgy and weld ability of stainless steels. John Wiley & Sons, 2011.